

Unraveling the Geologic History of the Hemlo Archean Gold Deposit, Superior Province, Canada: A U-Pb Geochronological Study

DONALD W. DAVIS†

Earth Sciences Dept., Royal Ontario Museum, 100 Queen's Park, Toronto, ON, Canada M5S 2C6

AND SHOUFA LIN

Department of Earth Sciences, University of Waterloo, Waterloo, ON, Canada N2L 3G1

Abstract

The Hemlo deposit is one of Canada's largest gold camps. Gold is both structurally and lithologically controlled, but shows unusual relationships relative to many other Archean lode deposits. Field evidence suggests that gold was emplaced within mechanical and chemical traps along a jog in a major sinistral shear zone, most likely during early formation of second-generation (G_2) structures, which represent the most intense phase of regional deformation. Mineralization was followed by amphibolite-facies regional metamorphism.

U-Pb geochronology has been carried out on zircons from rocks associated with the deposit, in order to determine the precise chronology of geologic events and their relationship to mineralization. Zircon populations are commonly affected by both inheritance and hydrothermal/metamorphic crystal growth. Meaningful and precise age information can only be determined by precise single zircon dating on rocks from a well constrained, structural, and stratigraphic context.

Gold is mostly found near the deformed contact between the Moose Lake quartz porphyry volcanic complex and stratigraphically underlying metasedimentary rocks. These rocks have been folded by a camp-scale, non-cylindrical F_2 fold. Zircon from the Moose Lake quartz porphyry is dominated by inheritance and gives ages that extend from ~2800 to ~2690 Ma. Metasedimentary rocks that underlie and overlie the Moose Lake porphyry show a much narrower range of provenance ages, and are dominated by 2,690- to 2,693-million-year-old zircon. Two detrital zircons from a metasedimentary rock directly beneath the porphyry define an age of 2685 ± 4 Ma. This should be an older age limit on volcanism, deformation, and gold mineralization. The four youngest near-concordant zircons from the Cedar Lake pluton define a magmatic age of 2680 ± 1 Ma. This pluton was emplaced prior to or early during G_2 deformation, while emplacement of gold was most likely controlled by G_2 structures. Therefore, 2680 ± 1 Ma probably also represents an older age limit on gold mineralization. A feldspar porphyry dike that cuts gold ore gives a younger age bracket of 2677 ± 1 Ma.

The results of zircon dating suggest that a volcanosedimentary complex was constructed in the area over the period of 2693 to 2685 Ma. This developed on earlier crust, ca. 2720 Ma in age, but there is evidence from detritus and xenocrysts for older rocks dating back to over 2800 Ma. Deposition of supracrustal rocks was followed by granodiorite plutonism at 2680 ± 1 Ma, then major deformation (G_2) and gold mineralization, overprinted by amphibolite-facies metamorphism (previously dated at 2676 Ma from titanite ages). Late-tectonic "sanukitoid suite" plutons were emplaced at 2677 ± 1 Ma. Thus, the primary gold-forming event occurred near the beginning of a period of plutonism and crustal reworking that lasted, at most, a few million years. This time association supports the view that granitoid magmas were the source of auriferous fluids. Plutons intruded into an actively deforming crust and were probably also the heat source for regional metamorphism. The most likely environment was a tectonically active, Timiskaming-type sedimentary basin. Similarly aged basins are found in the Timmins area to the east and the Shebandowan greenstone belt to the west.

Introduction

THE HEMLO gold deposit is located in the Hemlo-Heron Bay greenstone belt within the late Archean Superior province (Wawa subprovince). It is one of the largest gold deposits in Canada, containing over 20 Moz and hosting three active mines. Gold at Hemlo is disseminated in a high-strain zone, and ore-zone rocks underwent enrichment in Mo and K. Since its discovery in the early 1980s, it has been the focus of much controversy regarding the timing and cause of mineralization. Genetic models proposed for the deposit include mineralization by epithermal/syngenetic processes (Goldie, 1985; Valliant and Bradbrook, 1986), porphyry-related mineralization (Johnston and Smyk, 1992; Kuhns et al., 1994; Johnston, 1996), shear zone-related mineralization (Hugon, 1986;

Muir, 1993), and mineralization during late calc-silicate alteration (Pan and Fleet, 1995).

A precise knowledge of absolute age relationships is critical for understanding the primary setting of deformed and metamorphosed rocks in greenstone belts. Such knowledge is important for revealing the tectonic environment in which mineral deposits formed, and may be useful in targeting favorable areas for exploration. Most gold deposits in the Superior province appear to have formed relatively late in the history of their host greenstone belts. Although reliable older-age constraints can be established by dating the host rocks, gold mineralization is rarely cut by Archean igneous rocks. Therefore, younger-age constraints have often relied upon secondary hydrothermal mineral ages whose significance has been disputed (Corfu and Davis, 1991). Relative to other Archean lode gold deposits, mineralization at Hemlo is unusual in a

† Corresponding author: e-mail, dond@rom.on.ca

number of respects, but particularly in that it appears to have occurred before or early during regional deformation and metamorphism (Kuhns et al., 1994; Powell et al., 1999; Lin, 2001a). It is both hosted and cut by Archean felsic igneous rocks. Therefore, U-Pb dating holds the promise of precisely constraining the age of gold mineralization and revealing relationships to magmatism, metamorphism, and deformation.

As a result of a three-year project by the Canadian Mining Industry Research Organization (CAMIRO), the area of the deposit has received a detailed, multidisciplinary examination (Sutcliffe et al., 1998). This included structural field mapping (also published as Lin, 1998), geochemistry, geophysics, and geochronology. A parallel project by the Ontario Geological Survey was carried out on the regional structure, geochemistry, and geochronology of the Hemlo-Heron Bay greenstone belt (Jackson et al., 1998).

This paper presents results of the geochronological component of the CAMIRO project, supplemented by new data. It reports geochronological results from 14 samples, representing all major zircon-bearing lithologies in the area of the deposit. In combination with field-based stratigraphic and structural interpretations (Lin, 2001a), these data tightly constrain the timing and setting of mineralization.

Geologic Background

The Hemlo-Heron Bay greenstone belt trends east-west between two late Archean batholithic complexes, the Black Pic batholith to the north and the Pukaskwa intrusive complex to the south (Fig. 1). The greenstone belt is dominated by metavolcanic rocks in the west and metasedimentary rocks in the east, and is internally intruded by the Heron Bay and Cedar Lake granitoid plutons. Regional studies of geology, geochemistry, and geochronology are summarized in Jackson et al. (1998) and Beakhouse (2001). Supracrustal rocks are metamorphosed to grades that vary from upper greenschist facies in the west to amphibolite facies in the east (Jackson et al., 1998). Metamorphic grade is at amphibolite facies in the area of the gold deposit (Kuhns et al., 1994; Powell et al., 1999).

The Hemlo deposit area has been mapped in detail by previous workers (e.g., Muir, 1997; Lin, 2001a, and references therein; Lin, 2001b). As a result of the work by Lin (2001a), a lithostratigraphy for the deposit area was established (Figs. 2 and 3). The lowermost lithologic unit in the immediate area is basalt (map unit Ab), which is in sheared contact with metasedimentary rocks south of the deposit. The metasedimentary

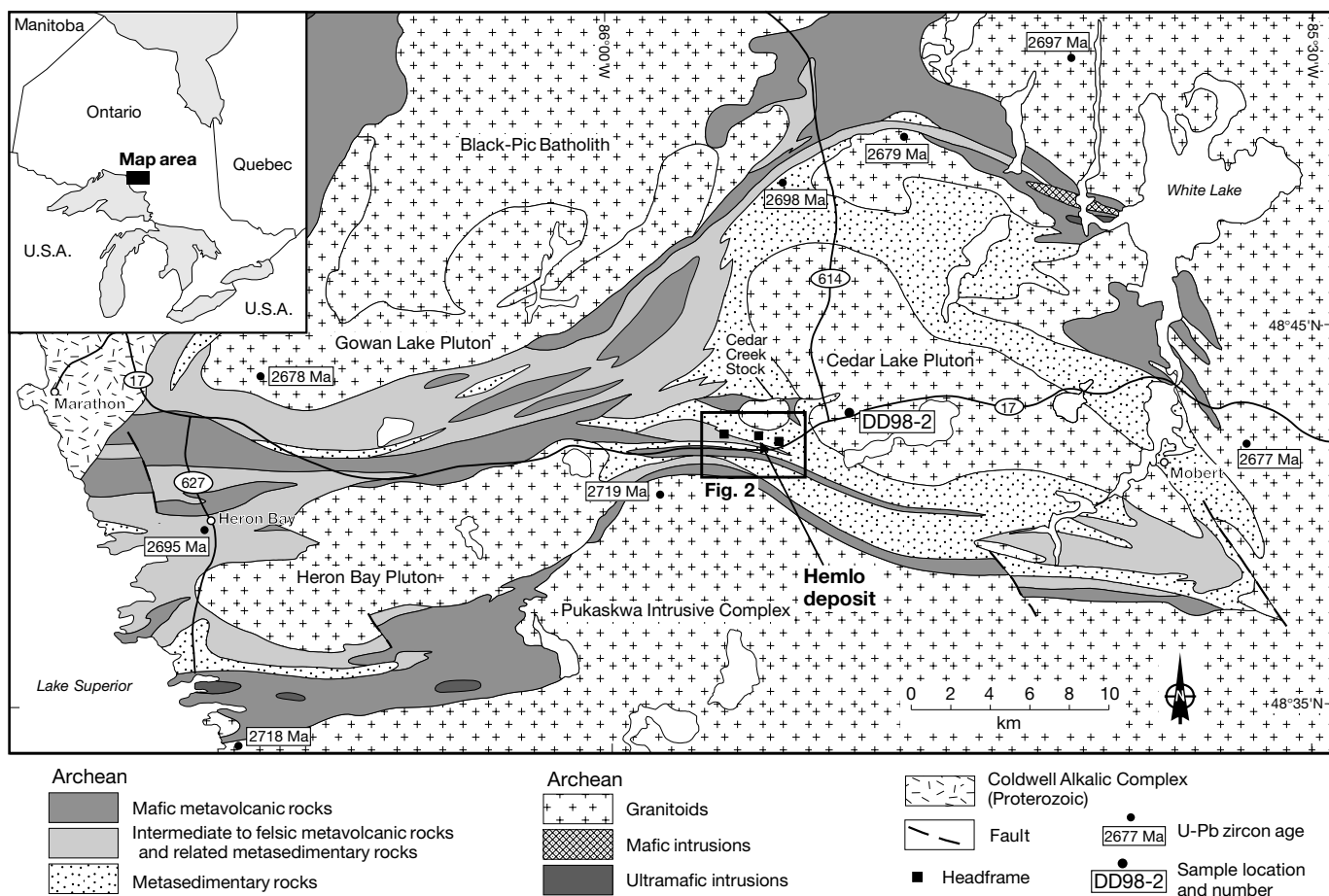
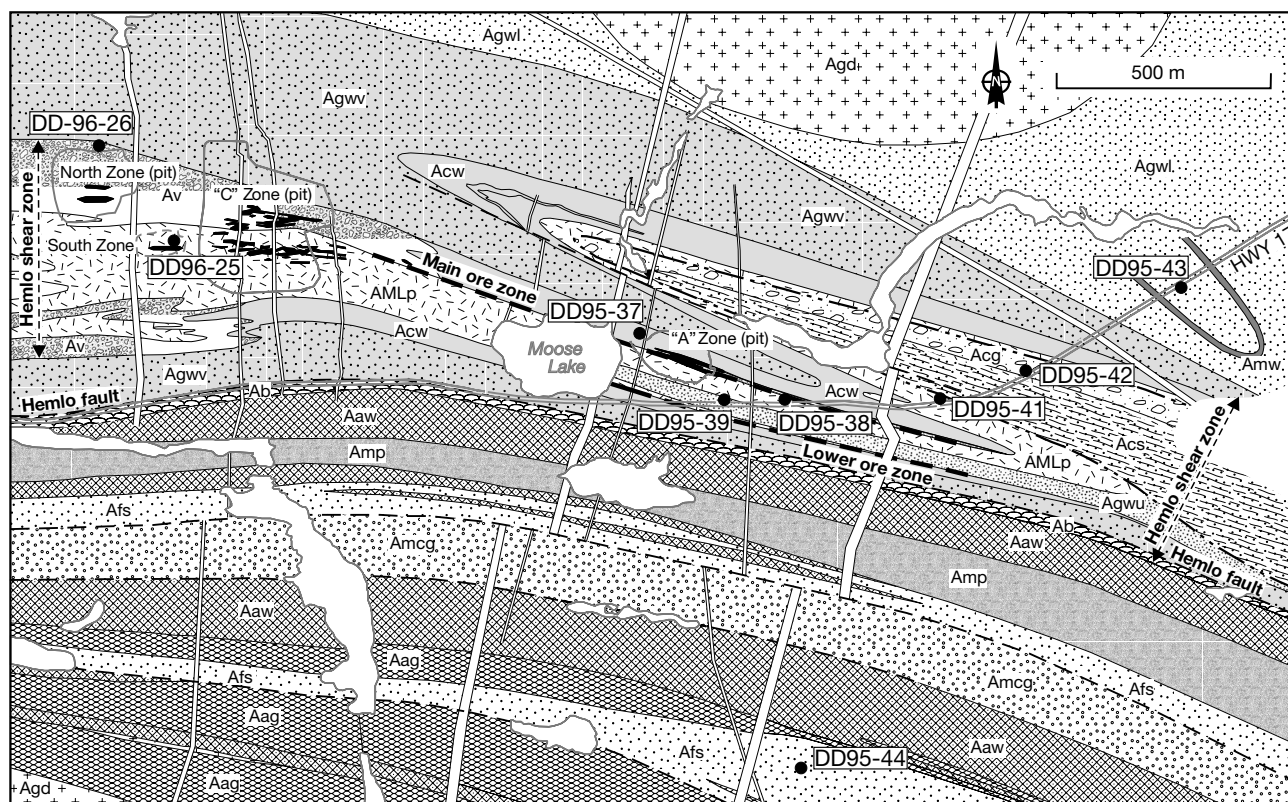

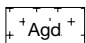


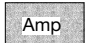

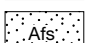
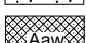

FIG. 1. Simplified geologic map of the Heron Bay-Hemlo greenstone belt, showing the regional geologic setting of the Hemlo gold deposit. Modified from Muir (1993), with U-Pb zircon ages from Corfu and Muir (1989a) and Jackson et al. (1998).



Intrusive rocks

-  Proterozoic diabase dikes
-  Archean granitoid intrusions

Archean supracrustal rocks south of the Hemlo shear zone

-  Metapelite and metagraywacke
-  Metaconglomerate
-  Felsic schist (quartz-feldspar schist)
-  Amphibole-rich metawacke
-  Amphibolitic gneiss, amphibolite

Archean Supracrustal rocks in and north of the Hemlo shear zone

(Arrow indicates stratigraphic order, from unit Ab to unit Acs)


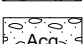
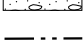

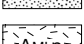
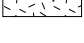


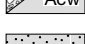
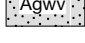
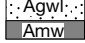


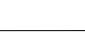
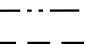
-  Cumingtonite schist
-  Heterolithic conglomerate and graywacke
-  Unconformity
-  Upper graywacke
-  Moose Lake porphyry (quartz +/- feldspar porphyry)
-  Surface gold mineralization/up-dip projection of ore zones
-  Sample location and number
-  Av: Reworked volcanoclastic rocks
-  Acw: Calc-silicate-band-rich wacke
-  Unit Agwl interlayered with unit Av.
-  Lower graywacke (Agwl), locally mafic (Amw)
-  Basalt (amphibolite)
-  Lithological contact
-  Unconformable contact
-  Brittle fault

FIG. 2. Geologic map of the immediate Hemlo deposit area, showing the locations of geochronological samples dated in this study. Note that the location of sample DD98-2 is shown in Figure 1. Simplified from part of a 1:10,000 scale geological map (Lin, 2001b).

rocks consist of lower feldspathic graywacke (Agwl) and reworked volcanoclastic rocks (Av). The latter grade laterally into graywacke with abundant calc-silicate bands (Acw), which probably represent metamorphosed calcareous pelitic horizons. These metasedimentary rocks are overlain by a quartz-feldspar porphyry complex known as the Moose Lake porphyry (AMLp). It shows fragmental textures and is interpreted to be volcanic in origin (e.g., Muir, 1997; Lin, 2001a, and references therein). The Moose Lake porphyry is conformably overlain by an upper graywacke (Agwu) with a more

mafic composition. Both these units appear to be unconformably overlain by heterolithic conglomerate and graywacke (Acg). The uppermost unit is a cumingtonite schist (Acs).

There are three major generations (G_1 to G_3) of ductile structures in the Hemlo area (Muir and Elliott, 1987; Lin, 2001a, and references therein). The connotation "G" is used instead of "D," as in Lin (2001a), because the three generations of structures (G) do not necessarily correspond to three discrete episodes of deformation (D). Structures are grouped into generations based on overprinting relationships and

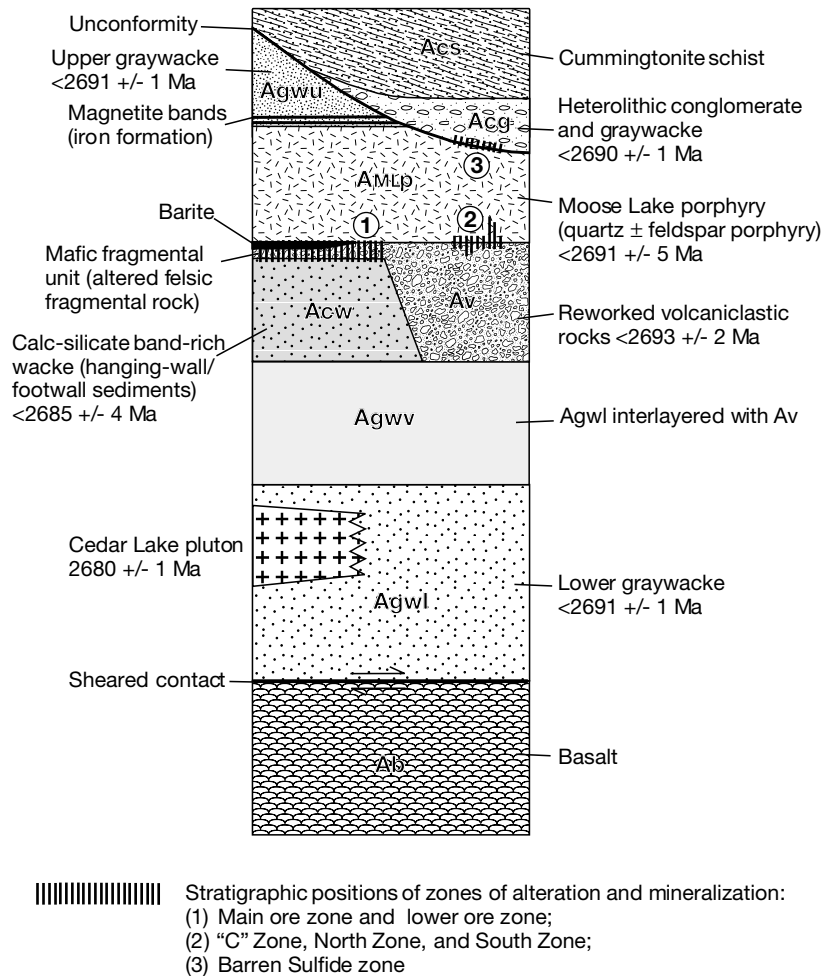


FIG. 3. Lithostratigraphy in the Hemlo deposit area from Lin (2001a). Age constraints from zircon geochronology are indicated. See Figure 2 for legend.

styles, and more than one generation of structures may develop in a single episode of progressive deformation. G_2 deformation, which overprints locally preserved G_1 structures, is the strongest and is interpreted by Lin (2001a) to have occurred in a regime of sinistral transpression. Macroscopic (camp-scale) F_2 folds dominate the geometry of the Hemlo camp. G_2 deformation is most intense in the 1-km wide Hemlo shear zone (Lin, 2001a). Widespread G_3 structures are related to regional dextral shearing. A fourth generation of brittle-ductile structures locally overprints the S_2 fabric.

The Hemlo gold deposit is found within the Hemlo shear zone, dominantly in an east-southeast-trending bend of the otherwise east-west-trending shear zone. The bulk of the ore occurs in two zones, the main and lower ore zones, which are located at the contact of the Moose Lake porphyry and an underlying wacke unit with calc-silicate bands (Acw , known as the hanging-wall and footwall sediments at the locations of the main and lower ore zones, respectively). This contact was folded during the main (G_2) phase of deformation (Fig. 2). A fragmental rock and a barite horizon occur at the contact. They appear to be the main protoliths of ore, and may have served as mechanical and chemical traps (Lin, 2001a, and references therein). Additional, but much less significant, ore is

also found within the Moose Lake porphyry and the hanging-wall metasedimentary rocks. The main phase of mineralization is interpreted to have occurred early during G_2 or before G_2 (most likely early during G_2), and before peak amphibolite-facies metamorphism, which took place late during G_2 or between G_2 and G_3 (Lin, 2001a). In contrast, Powell et al. (1999) suggested that kyanite formation during peak regional metamorphism predates the main D_2 fabric, but postdates mineralization. However, it is not clear whether the D_2 of Powell et al. is equivalent to Lin's G_2 . Mineralization involved introduction of Au, S, Mo, Zn, As, Sb, Hg, Tl, and W, and pervasive potassic alteration. This was followed by three post- G_2 remobilization events that produced, in chronological order, secondary Au-Sb-Si, Au-Ca, and Au-As-Hg mineralization (Sutcliffe et al., 1998). The deposit is intruded by a swarm of foliation-parallel feldspar porphyry dikes.

Earlier work on the geochronology of the Hemlo area was done by Corfu and Muir (1989a, b). A marginal granodiorite phase of the Pukaskwa gneissic complex was dated at 2719^{+6}_{-3} Ma. A felsic volcanic unit near Heron Bay was found to be $2,695 \pm 2$ Ma in age. Ages of about 2688 Ma were reported for phases of the Cedar Lake pluton, the Heron Bay pluton, and an internal phase of the Pukaskwa complex. The Gowan

Lake pluton was found to be the youngest body at 2678 ± 2 Ma. Within the altered zone associated with the gold deposit, an age of 2772 ± 2 Ma was reported on a phase of the Moose Lake porphyry, whereas more poorly defined ages in the range of 2680 to 2695 Ma were interpreted for dikes, one of which intruded ore. Titanite from a number of plutons outside the deposit gave overlapping ages of 2677 ± 1 Ma, whereas titanite from rocks within the deposit gave slightly younger ages of about 2671 ± 1 Ma. Powell et al. (1999) suggested that the earlier age represents peak kyanite-grade metamorphism at 6 to 7 kbars and 600° to 650°C , while the later titanite may record a sillimanite overprint at similar temperature but lower pressure (4–5 kbars). These may represent parts of a single progressive metamorphic process. Rutile and monazite in altered units gave much younger ages in the range of 2645 to 2632 Ma. Pan and Fleet (1995) suggested that these minerals date hydrothermal activity associated with gold. However, others suggested that they record late hydrothermal activity associated with remobilization of gold or closure to diffusion of Pb during slow cooling (Corfu and Muir, 1989b; Powell et al., 1999).

Johnston (1996) reported unpublished data from H. Wasteneys, that show that the Moose Lake porphyry contains a complex pattern of zircon ages dominated by inheritance, in the range of ca. 2700 to 2800 Ma. In addition, two highly discordant data from the Kusun's porphyry, which cuts gold mineralization, define an age of 2680 ± 10 Ma.

Analytical Methods

Sample processing and U-Pb geochronology followed standard procedures practiced at the Royal Ontario Museum laboratory (Krogh, 1973; Corfu and Muir, 1989a). Most rock samples weighed about 10 kg and yielded abundant zircon, except the dikes, which yielded only a small amount of zircon. Exterior surfaces of selected zircon grains were removed by air abrasion (Krogh, 1982). Because of the age complexity of samples from the Hemlo deposit and the rarity of fresh zircon, only single-grain analyses on abraded zircons were carried out. Weights of grains were estimated by eye, a process that is usually accurate to about ± 50 percent. This affects only U and Pb concentrations, not age information, which depends only on isotopic ratio measurements. Some samples, weighing a few micrograms or less, were loaded directly into the mass spectrometer after dissolution and without chemistry. Pb and U were loaded together on Re filaments using silica gel, and analyzed with a VG354 mass spectrometer. Most of the measurements were made using a Daly collector with a constant detector mass discrimination of 0.40 percent/amu. Thermal mass discrimination corrections are 0.10 percent/amu.

Th/U was determined on some whole rocks to compare with zircon. These analyses were carried out at the Geological Survey of Canada.

Results

Results from 14 samples are reported here. Sample locations are shown on Figure 2 or indicated below. Images of selected zircon populations are given in Figure 4. Results of isotopic measurements are given in Table 1 (errors are at 2σ) and are plotted on Figures 5 to 7. Abraded zircons to be analyzed

were selected to be free of cracks and alteration. Low blank analyses of unaltered concordant zircon by isotopic dilution, as well as high-temperature Pb evaporation and ion microprobe measurements, show that zircon generally crystallizes with negligible quantities of initial lead. Therefore, all measured common lead is assumed to have the isotopic composition of the laboratory blank (see footnotes to Table 1). Excess common Pb can be introduced into zircon by alteration, but this is usually associated with significant discordance (Krogh and Davis, 1974, 1975). With one exception (sample DD95-41; see below), variations in common Pb from near-concordant data are likely due to minor fluctuations in handling blank, which is difficult to maintain constant at the picogram level.

The weighted mean of near-concordant data with overlapping $^{207}\text{Pb}/^{206}\text{Pb}$ ages was determined by calculating a regression line through the data, forced through the origin of concordia, using the method of Davis (1982). Probabilities of fit are expected to be about 50 percent on average if analytical errors have been correctly assigned and there is no scatter from multi-aged components. This procedure gives the same ages, errors, and probabilities of fit as direct weighted mean calculations given by the Isoplot program (Ludwig, 1998). Age errors in the text and figures are quoted at the 95 percent confidence level. Error ellipses in the figures are given at the 2σ level. Samples are grouped below and in Table 1, according to whether they are most closely related to metavolcanic, metasedimentary, or intrusive (dike) rocks. Detailed descriptions of the units sampled are given in Lin (2001a).

Correct interpretation of rock emplacement ages from zircon ages can be difficult in cases where there is extensive inheritance from older zircon and/or subsolidus growth of metamorphic or hydrothermal zircon. Both problems are present in many of the rocks from the Hemlo area. Use is made of calculated Th/U ratios in zircon (from $^{206}\text{Pb}/^{208}\text{Pb}$ measurements) in distinguishing metamorphic/hydrothermal zircon (low Th/U; Rubatto, 2002) from magmatic zircon (Th/U > 0.1). Measurements of Th/U in magmatic zircon and host rocks from granitoid bodies in the Hemlo belt indicate that zircon fractionates Th/U by about 0.1, relative to its host magma (Jackson et al., 1998). This can be used to help distinguish xenocrystic from magmatic zircon. In cases of magmatic inheritance, the youngest near-concordant data should give an older estimate on emplacement of the rock. Because of these complexities, previously published data have in some cases been reexamined and reinterpreted (see below).

Metavolcanic and quartz porphyry-related samples

DD95-38 Mineralized fragmental Moose Lake porphyry, map unit AMLp (Fig. 5A): This sample, from the ore exposure at Highway 17 (field trip stop 20A of Muir et al., 1991), contains a large amount of barite. Because barite is nonmagnetic and of the same density as zircon, it is concentrated with the best zircon fractions, making it difficult to recover the zircon by hand picking. Since barite is a relatively soft mineral, most of it was removed by abrading small fractions of the concentrate for 1 to 2 h. By doing this over a period of several days, a pure zircon fraction was prepared from half of the dense, nonmagnetic fraction. Unfortunately, the abrasion process slightly rounded all of the zircon grains and made it

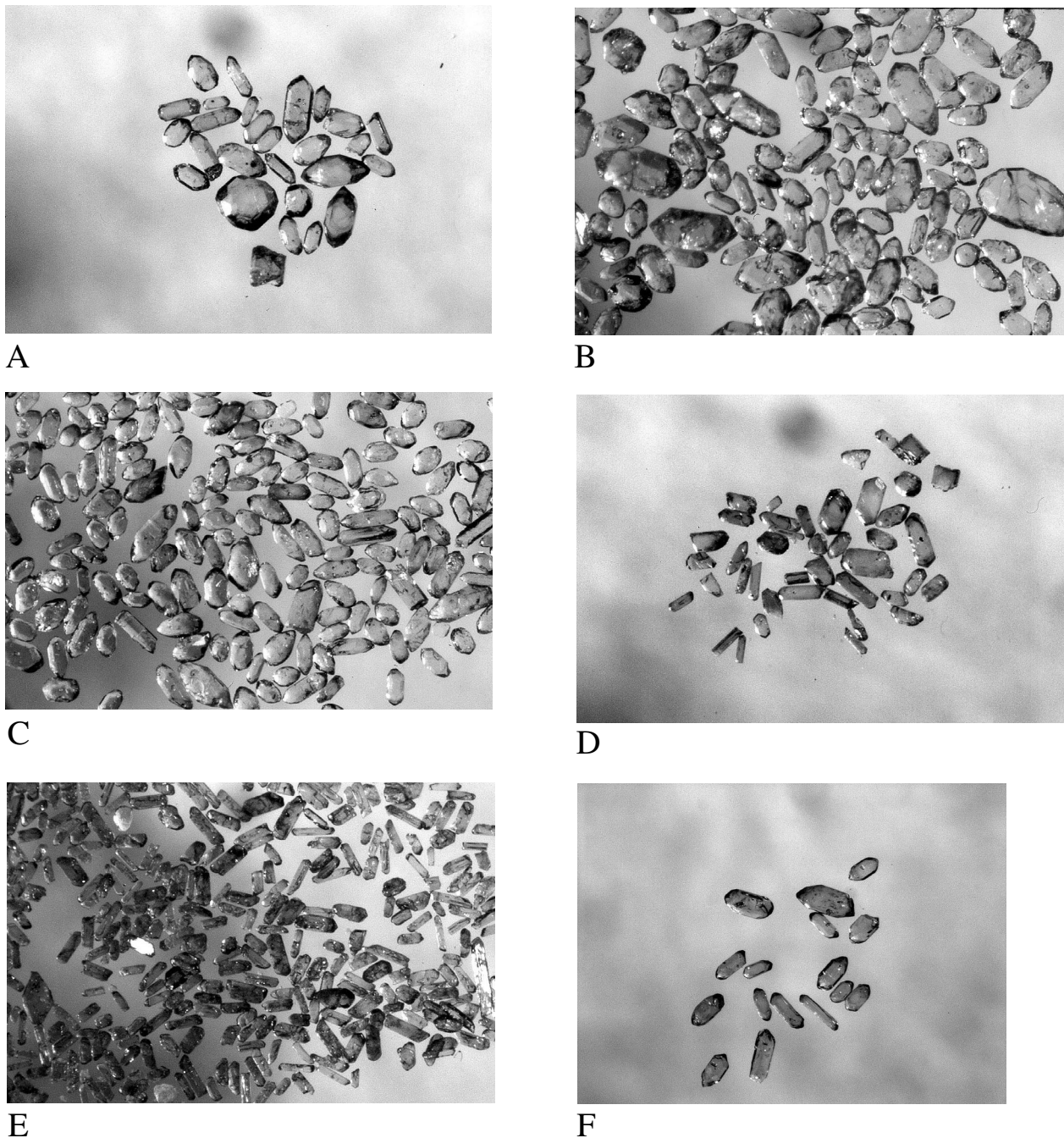


FIG. 4. Photomicrographs of zircon picked from: A. DD96-25 Moose Lake porphyry (unit AMLp). B. DD95-43 Lower graywacke (unit Agvl). C. DD96-26 Felsic reworked volcanoclastic rock (unit Av). D. LIN97-1 Feldspar porphyry dike cutting ore. E. LIN97-2 Mineralized aplite dike. F. DD98-2 Cedar Lake pluton. Field of view has a width of 2 mm.

impossible to tell which grains had a primary euhedral shape. Eight zircon grains selected as having slightly different colors and inclusion types gave a wide range of $^{207}\text{Pb}/^{206}\text{Pb}$ ages, from 2694 ± 2 to 2813 ± 2 Ma. The youngest grain gives an older age limit on deposition of the fragmental porphyry and on gold mineralization.

DD96-25 Fragmental Moose Lake quartz porphyry at South zone, map unit AMLp (Fig. 5B): The population is dominated by highly cracked, euhedral, short prismatic, and

stubby grains with well developed secondary crystal faces, similar to morphological types S12 to P3 defined by Pupin (1980). A few grains have visible cores, but cores are not obvious in most of the population. Grains that showed no visible evidence of cores were picked for abrasion (Fig. 4A). Seven of these gave a scattered data set indicating the presence of inheritance. The results suggest an age of around 2800 Ma for the inherited components, but the emplacement age of the porphyry is unclear.

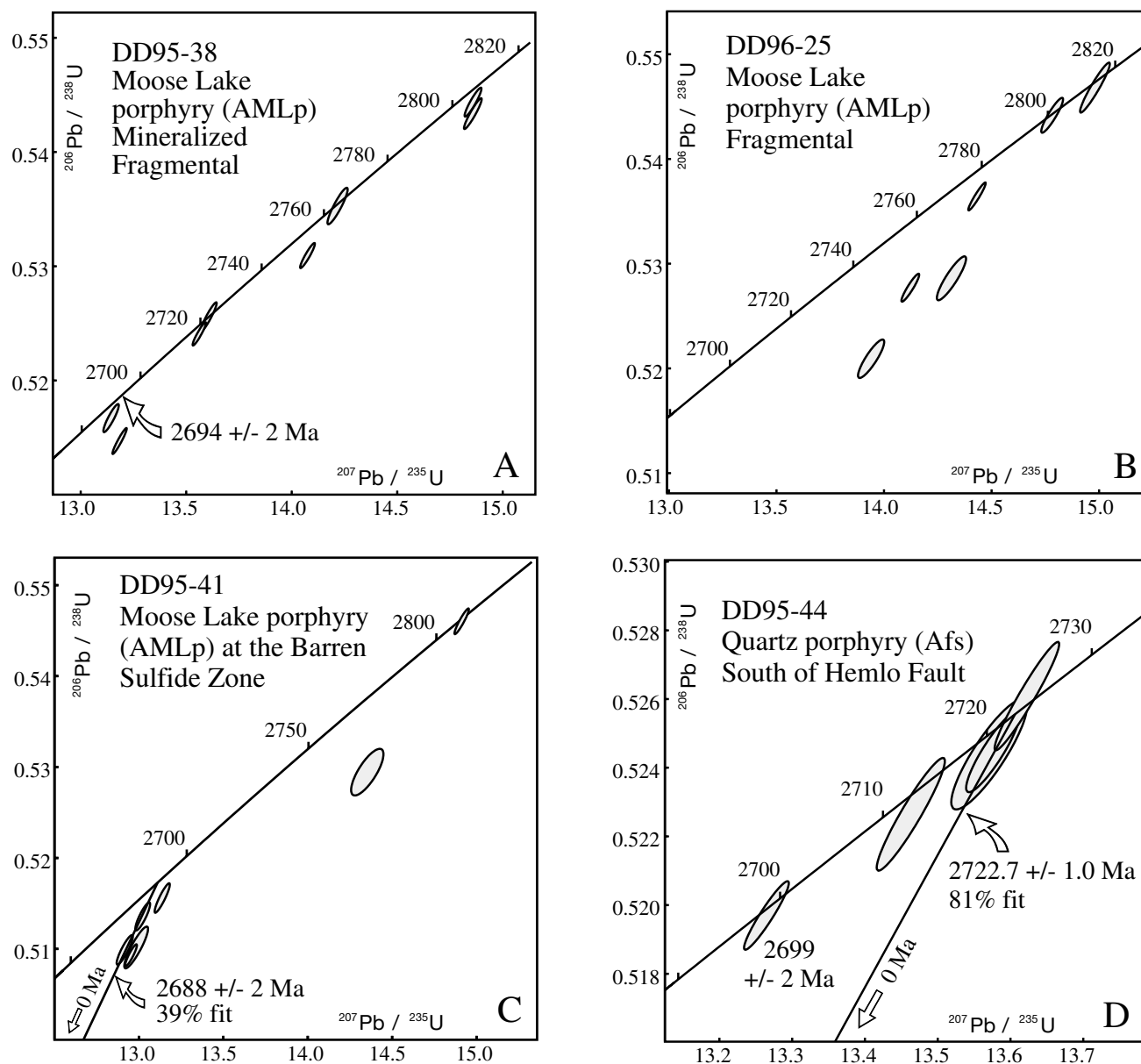


FIG. 5. U-Pb concordia plots showing data on single zircons from quartz porphyries in the Hemlo area.

DD95-41 Barren Sulfide zone porphyry, map unit AMLp (Fig 5C): This unit was mapped as reworked felsic detritus by Muir (1997), but is interpreted as part of the Moose Lake porphyry by Lin (2001a). Zircons within this sample are quite diverse in appearance. Colors vary from brownish to colorless, and morphologies, from euhedral to well rounded. One batch of analyses from this rock has an unusually high Pb blank. This contaminant was traced to a particular acid bottle and the isotopic composition of the blank was precisely measured ($^{206}\text{Pb}/^{204}\text{Pb} = 19.587 \pm 0.039$, $^{207}\text{Pb}/^{204}\text{Pb} = 15.713 \pm 0.031$, $^{208}\text{Pb}/^{204}\text{Pb} = 38.84 \pm 0.16$), so the age errors are not seriously increased. Two data, one of which is concordant, give ages of around 2800 Ma. The younger data are slightly discordant and vary in the range of 2697 to 2687 Ma. There was no obvious relationship between age and zircon color or

morphology, in this sample or the others. The two youngest data give overlapping $^{207}\text{Pb}/^{206}\text{Pb}$ ages, with an average of 2688 ± 2 Ma. These show different Th/U ratios, so the zircons may have been from different sources, but they provide an estimated older age limit on emplacement of the porphyry.

DD95-44 Quartz porphyry (Afs) South of Hemlo fault, map unit Afs (Fig. 5D): Zircons from this sample are stubby and multifaceted. Most appear to be slightly subrounded. Well rounded grains are rare. Many zircons are slightly brownish and have abundant rod and bubblelike inclusions. Analyses of three grains with characteristics typical of the main population gave overlapping data, with an average age of 2723 ± 1 Ma. However, the youngest concordant datum gives an age of 2699 ± 2 Ma, which is an older age limit on emplacement of the porphyry.

TABLE 1. U-Pb Isotope Data for Single Zircons from the Area of the Hemlo Gold Deposit

No.	Description	Wt (mg)	U (ppm)	Th/U	PbCom (pg)	²⁰⁷ Pb/ ²⁰⁴ Pb	²⁰⁶ Pb/ ²³⁸ U	2σ	²⁰⁷ Pb/ ²³⁵ U	2σ	²⁰⁷ Pb/ ²⁰⁶ Pb	2σ	Disc. (%)
<u>Volcanic and quartz porphyritic rocks</u>													
<u>1</u>	DD95-38 Mineralized fragmental Moose Lake porphyry, map unit AMLp, highway 17: 580658mE, 5393497mN												
1	1 Ab zr, clr, incl	0.007	34	0.48	1.1	1551	0.5434	0.0014	14.858	0.042	2812.5	1.6	0.7
2	1 Ab zr, clr, incl	0.005	40	0.44	1.2	1164	0.5444	0.0013	14.859	0.040	2809.6	1.7	0.3
3	1 Ab zr, brn	0.001	142	0.42	1.5	639	0.5353	0.0016	14.217	0.048	2764.8	2.3	0.1
4	1 Ab zr, clr	0.015	17	0.23	1.3	1377	0.5309	0.0011	14.075	0.035	2761.6	1.5	0.7
5	1 Ab zr, brn, rnd	0.004	63	1.27	1.23	1316	0.5256	0.0013	13.606	0.038	2722.7	1.6	0.0
6	1 Ab zr brn, incl	0.002	379	0.49	0.9	3938	0.5241	0.0010	13.562	0.032	2722.0	1.4	0.2
7	1 Ab zr, brn	0.003	192	0.27	1.4	2540	0.5147	0.0011	13.184	0.034	2705.2	1.4	1.3
8	1 Ab zr, clr, rnd	0.002	89	0.85	1.3	846	0.5167	0.0012	13.144	0.037	2693.7	1.9	0.4
<u>2</u>	DD96-25 Fragmental Moose Lake porphyry, map unit AMLp, South Zone outcrop: 578474mE, 5394067mN												
1	1 Ab zr, euh, clr	0.001	57	0.59	0.6	685	0.5468	0.0024	14.981	0.069	2815.5	2.4	0.2
2	1 Ab zr, euh, clr	0.001	64	0.42	0.7	669	0.5442	0.0017	14.782	0.051	2801.6	2.3	0.0
3	1 Ab zr, euh, clr	0.010	17	0.39	1.9	643	0.5286	0.0021	14.314	0.068	2796.4	3.5	2.7
4	1 Ab zr, euh, clr	0.020	25	0.34	1.1	2951	0.5364	0.0013	14.432	0.040	2785.9	1.4	0.8
5	1 Ab zr, euh, clr	0.005	33	0.36	1.2	925	0.5277	0.0013	14.122	0.041	2777.2	1.8	2.0
6	1 Ab zr, euh, clr	0.001	91	0.46	2.2	286.7	0.5209	0.0018	13.940	0.061	2777.1	3.5	3.3
<u>3</u>	DD95-41 Moose Lake porphyry at the Barren Sulfide zone, map unit AMLp, highway 17: 581270mE, 5393503mN												
1	1 Ab euh clr zr, no incl	0.002	101	0.35	0.6	2355	0.5460	0.0014	14.912	0.043	2810.3	1.7	0.1
2	1 Ab zr	0.001	50	0.36	8.3	56.49	0.5294	0.0026	14.353	0.096	2798.3	7.0	2.6
3	1 Ab euh zr	0.0015	72	0.54	0.8	823.2	0.5156	0.0016	13.138	0.045	2696.5	2.3	0.7
4	1 Ab euh zr, incl	0.002	135	0.39	1.2	1413	0.5093	0.0012	12.953	0.035	2693.4	1.8	1.8
5	1 Ab zr frag	0.002	40	0.52	8.5	73.44	0.5102	0.0023	12.984	0.070	2694.5	4.1	1.7
6	1 Ab zr, brn, rod incl	0.001	170.2	0.83	9.0	131.97	0.5136	0.0015	13.023	0.044	2688.4	2.7	0.8
7	1 Ab zr, brn	0.0005	244.8	0.24	9.1	97.99	0.5099	0.0016	12.916	0.048	2686.7	2.8	1.4
<u>4</u>	DD95-44 Quartz porphyry south of Hemlo fault, map unit Afs: 580908mE, 5392075mN												
1	1 Ab zr, brn, euh, incl	0.003	133	0.48	1.1	2223	0.5261	0.0016	13.623	0.044	2723.0	1.5	-0.1
2	1 Ab zr, brn, euh, incl	0.003	68	0.60	1.3	1027	0.5245	0.0012	13.576	0.037	2722.4	2.0	0.2
3	1 Ab zr, brn, euh	0.002	41	0.98	1.6	345.5	0.5244	0.0016	13.571	0.052	2722.0	3.2	0.2
4	1 Ab zr, clr, euh	0.006	31	0.40	1.5	767.6	0.5226	0.0016	13.463	0.047	2714.4	1.9	0.2
5	1 Ab zr clr, euh	0.015	72	0.43	1.3	5170	0.5197	0.0010	13.265	0.031	2699.2	1.3	0.1
<u>Metasedimentary rocks</u>													
<u>5</u>	DD95-43 Lower graywacke, map unit Agwl, highway 17: 582123mE, 5393912mN												
1	1 Ab zr, no incl	0.002	81	0.42	1.0	972	0.5178	0.0013	13.208	0.039	2698.1	1.8	0.4
2	1 Ab zr, clr incl	0.010	39	0.35	1.5	1624	0.5182	0.0012	13.211	0.036	2697.4	1.6	0.3
3	1 Ab zr, incl	0.010	51	1.23	1.8	1739	0.5163	0.0011	13.109	0.032	2690.7	1.5	0.3
4	1 Ab zr, incl	0.004	125	0.78	3.1	991	0.5153	0.0011	13.085	0.034	2690.6	1.7	0.5
5	1 Ab zr, clr incl	0.005	88	0.81	1.7	1611	0.5174	0.0012	13.134	0.036	2690.1	1.6	0.1
<u>6</u>	DD95-39 Upper graywacke, map unit Agwu, highway 17: 580493mE, 5393496mN												
1	1 Ab zr, rnd	0.006	30	0.52	0.9	1321	0.5191	0.0012	13.361	0.035	2713.1	1.6	0.8
2	1 Ab subrnd zr, incl	0.002	327	1.62	1.4	2771	0.5157	0.0016	13.097	0.044	2691.0	1.7	0.5
3	1 Ab euh zr, clr incl	0.010	109	0.92	1.5	4234	0.5176	0.0014	13.138	0.038	2690.3	2.1	0.1
4	1 Ab euh zr, no incl	0.001	267	1.05	1.0	1661	0.5168	0.0016	13.118	0.043	2690.2	2.2	0.2
5	1 Ab subrnd zr, no incl	0.006	111	0.86	2.3	1729	0.5162	0.0018	13.102	0.047	2689.9	2.3	0.3
<u>7</u>	DD96-26 Reworked felsic volcanoclastic rock, north wall of the North Zone pit, map unit Av: 578198mE, 5394419mN												
1	1 Ab zr, clr, euh, incl	0.001	105	0.48	1.1	571.3	0.5040	0.0017	12.821	0.049	2693.9	2.5	2.9
2	1 Ab zr, clr, euh	0.001	27	0.45	0.6	285.7	0.5190	0.0017	13.202	0.059	2693.8	4.4	0
3	1 Ab zr, clr, euh, incl	0.001	39	0.44	1.2	203.7	0.4716	0.0021	11.988	0.068	2692.4	5.1	9
4	1 Ab zr, clr, euh	0.0005	63	0.39	0.5	419.1	0.5180	0.0018	13.165	0.055	2692.2	3.1	0.1
5	1 Ab zr, clr, euh, incl	0.002	31	0.47	1.4	278.5	0.4969	0.0017	12.619	0.056	2691.1	4.4	4.1
6	1 Ab zr, clr, euh, incl	0.001	19	0.46	0.8	145.0	0.4589	0.0034	11.643	0.105	2689.2	7.2	11.3
<u>8</u>	DD95-37 Hanging-wall sediments (metawacke), entrance to 'A' zone pit, map unit Acw: 580157mE, 5393738mN												
1	1 Ab zr, brn, crks & incl	0.0030	141	0.59	0.4	6207.1	0.5168	0.0017	13.160	0.044	2695.4	2.1	0.4
2	1 Ab zr, eq, melt incl	0.0060	16	0.59	0.3	1860.1	0.5182	0.0024	13.184	0.063	2693.9	2.3	0.1
3	1 Ab euh zr, brnsh, spr	0.0015	47	0.42	0.4	1127.8	0.5187	0.0018	13.197	0.045	2693.9	3.9	0.0
4	1 Ab euh zr, clr, flat	0.0030	14	0.62	0.4	713.7	0.5179	0.0024	13.174	0.065	2693.6	3.6	0.1
5	1 Ab zr, clr, lpr	0.0008	42	0.62	0.4	568.2	0.5181	0.0019	13.176	0.055	2693.4	2.6	0.1

TABLE 1. (Cont.)

No.	Description	Wt (mg)	U (ppm)	Th/U	PbCom (pg)	$^{207}\text{Pb}/^{204}\text{Pb}$	$^{206}\text{Pb}/^{238}\text{U}$	2σ	$^{207}\text{Pb}/^{235}\text{U}$	2σ	$^{207}\text{Pb}/^{206}\text{Pb}$	2σ	Disc. (%)
6	1 Ab zr, brn, euh	0.0004	176	0.45	0.5	949.6	0.5171	0.0026	13.150	0.069	2693.2	2.4	0.3
7	1 Ab euh zr, spr	0.0010	55	0.44	0.4	936.3	0.5187	0.0018	13.188	0.049	2693.0	2.6	0.0
8	1 Ab zr, brn, euh	0.0005	180	0.51	0.4	1377	0.5187	0.0017	13.186	0.047	2692.6	2.1	0.0
9	1 Ab zr, clr, euh	0.0010	43	0.64	1.4	204.5	0.5186	0.0030	13.184	0.089	2692.6	5.0	0.0
10	1 Ab zr, clr, euh	0.0005	158	0.39	0.6	889.6	0.5186	0.0017	13.184	0.048	2692.5	2.4	0.0
11	1 Ab zr, clr, euh, incl	0.0015	23	0.60	1.1	210.9	0.5167	0.0023	13.077	0.082	2685.2	6.2	0.0
12	1 Ab zr, clr, euh	0.0010	45	0.72	2.0	154.9	0.5173	0.0021	13.096	0.082	2685.7	6.6	-0.1
9	DD95-42 Heterolithic conglomerate, map unit Acg, highway 17: 581602mE, 5393627mN												
1	1 Ab rnd zr, lpr	0.0050	33	0.61	0.9	1241.4	0.5392	0.0018	14.716	0.052	2809.5	2.3	1.3
2	1 Ab zr, euh	0.0100	11	0.63	2.1	358.9	0.5265	0.0020	13.684	0.057	2729.1	4.9	0.1
3	1 Ab euh zr, rod incl	0.0050	18	0.57	0.6	894.6	0.5179	0.0019	13.195	0.053	2696.3	2.7	0.3
4	1 Ab euh zr, melt incl	0.0200	19	0.68	1.2	1895.0	0.5174	0.0016	13.180	0.044	2695.9	2.5	0.3
5	1 Ab zr, euh, clr, lpr	0.0005	34	0.56	0.4	289.7	0.5163	0.0018	13.135	0.064	2694.0	4.4	0.5
6	1 Ab euh zr, spr	0.0020	28	0.42	0.6	563.9	0.5180	0.0025	13.165	0.069	2692.2	3.2	0.1
7	1 Ab zr, brn to clr, flat	0.0010	226	0.38	0.5	3004.8	0.5119	0.0018	12.991	0.048	2689.7	2.2	1.1
8	1 Ab zr, brn, zoned	0.0010	314	0.55	0.4	4680.4	0.5156	0.0013	13.081	0.036	2689.3	2.1	0.4
Dikes and plutons													
10	LIN97-1 Feldspar porphyry dike intruding ore, hanging-wall contact, David Bell mine, C zone, level 11C, crosscut K3												
1	1 Ab zr, clr, elong, incl	0.003	27	0.45	1.3	362.5	0.4913	0.0017	12.453	0.050	2687.8	3.1	5.0
2	1 Ab zr, clr, flat	0.002	135	0.01	1.4	1172.7	0.5145	0.0013	13.013	0.038	2684.1	1.6	0.4
3	1 Ab zr, brn	0.003	81	0.23	1.3	1134.5	0.5143	0.0012	12.954	0.035	2677.4	1.6	0.1
4	1 Ab zr, brn, lpr	0.002	80	0.38	1.2	780.8	0.5074	0.0013	12.776	0.037	2676.8	2.0	1.4
5	1 Ab zr, brn	0.001	81	0.33	1.8	263.4	0.4754	0.0015	11.950	0.051	2674.1	4.0	7.5
11	DD96-23 Kusin's porphyry intruding sericitic ore: Golden Giant mine, level 4633, crosscut Q15												
1	1 Ab zr, lpr	0.0004	47	0.6	0.5	261.3	0.5368	0.0015	14.377	0.065	2778.5	4.6	0.4
2	1 Ab zr, brn	0.001	78	0.97	0.4	1113	0.5163	0.0017	13.129	0.046	2693.0	2.3	0.4
3	1 Ab zr, clr	0.0003	26	0.61	0.4	135.6	0.5161	0.0025	13.110	0.130	2691.2	11.5	0.4
4	1 Ab zr, brn	0.0003	68	0.56	0.5	244.9	0.5154	0.0030	13.081	0.089	2690.1	6.0	0.5
5	1 Ab zr	0.0004	66	0.02	0.5	338.4	0.5131	0.0016	12.898	0.058	2674.1	4.2	0.2
6	1 Ab zr, clr, lpr	0.0003	66	0.02	0.5	243.1	0.5127	0.0022	12.867	0.067	2671.5	4.6	0.2
7	1 Ab zr, cracks	0.0004	83	0.0	1.9	116.1	0.4986	0.0021	12.490	0.095	2668.2	9.2	2.7
12	DD97-25 Kusin's porphyry, sample 2, Golden Giant mine, level 4700, crosscut Q12												
1	1 Ab zr, clr, cracked	0.0010	164	0.04	0.4	2543.5	0.5141	0.0017	12.964	0.046	2679.2	2.3	0.2
2	1 Ab zr, brn, cracked	0.0010	188	0.05	0.4	2668.5	0.5080	0.0014	12.805	0.038	2678.5	2.2	1.4
3	1 Ab zr, brn, cracked	0.0005	174	0.04	0.3	1535.1	0.5135	0.0013	12.937	0.035	2677.7	2.3	0.3
4	1 Ab zr, brn, cracked	0.0005	186	0.03	0.3	1669.8	0.5070	0.0013	12.748	0.035	2674.7	2.3	1.4
13	LIN97-2 Mineralized aplite dike, David Bell mine, C zone, level 10A, crosscut K1												
1	1 Ab zr, equant	0.0005	112	0.02	0.5	706.9	0.5104	0.0014	12.859	0.041	2677.7	2.3	0.9
2	1 Ab zr, lpr	0.0005	188	0.0	1.9	312.4	0.5124	0.0014	12.905	0.046	2677.0	3.4	0.5
3	1 Ab zr, lpr	0.0005	115	0.01	0.5	650.7	0.5091	0.0019	12.813	0.054	2676.2	3.3	1.1
14	DD98-2 Cedar Lake pluton, map unit Agd, highway 17: 585041mE, 5395434mN												
1	1 Ab clr, euh, spr	0.0010	40	0.67	0.9	300.8	0.5234	0.0026	13.469	0.074	2712.6	3.6	0.0
2	1 Ab zr, euh, spr, pink	0.0020	35	0.75	0.6	765.5	0.5164	0.0044	13.098	0.112	2688.8	2.3	0.2
3	1 Ab clr, euh, spr	0.0010	54	0.66	0.2	1706.3	0.5162	0.0017	13.080	0.047	2687.4	1.9	0.2
4	1 Ab zr, euh, spr, pink	0.0050	24	0.64	0.6	1332.0	0.5122	0.0023	12.952	0.060	2683.9	2.6	0.8
5	1 Ab zr, tip, cracks	0.0010	121	0.43	2.1	354.1	0.5122	0.0023	12.926	0.063	2680.6	3.2	0.7
6	1 Ab zr, tip, brn, pink	0.0030	70	0.40	0.5	2782.7	0.5115	0.0014	12.907	0.039	2680.4	1.6	0.8
7	1 Ab clr, euh, spr	0.0005	70	0.36	0.2	967.5	0.5150	0.0023	12.991	0.060	2679.7	2.4	0.1
8	1 Ab zr, tip, cracks	0.0015	86	0.45	5.1	167.7	0.5152	0.0069	12.981	0.182	2677.8	6.6	0.0

Ab = abraded, brn = brownish, clr = colorless, euh = euhedral, incl = inclusions, lpr = long prismatic, rnd = rounded, spr = short prismatic, zr = zircon grain

PbCom = Common Pb, assuming all has isotopic composition of blank; $^{206}\text{Pb}/^{204}\text{Pb} = 18.221$; $^{207}\text{Pb}/^{204}\text{Pb} = 15.612$; $^{208}\text{Pb}/^{204}\text{Pb} = 39.36$ (2% errors)

Th/U calculated from radiogenic $^{208}\text{Pb}/^{206}\text{Pb}$ ratio and $^{207}\text{Pb}/^{206}\text{Pb}$ age assuming concordance

Disc = percent discordance for the given $^{207}\text{Pb}/^{206}\text{Pb}$ age

Decay constants are from Jaffey et al. (1971)

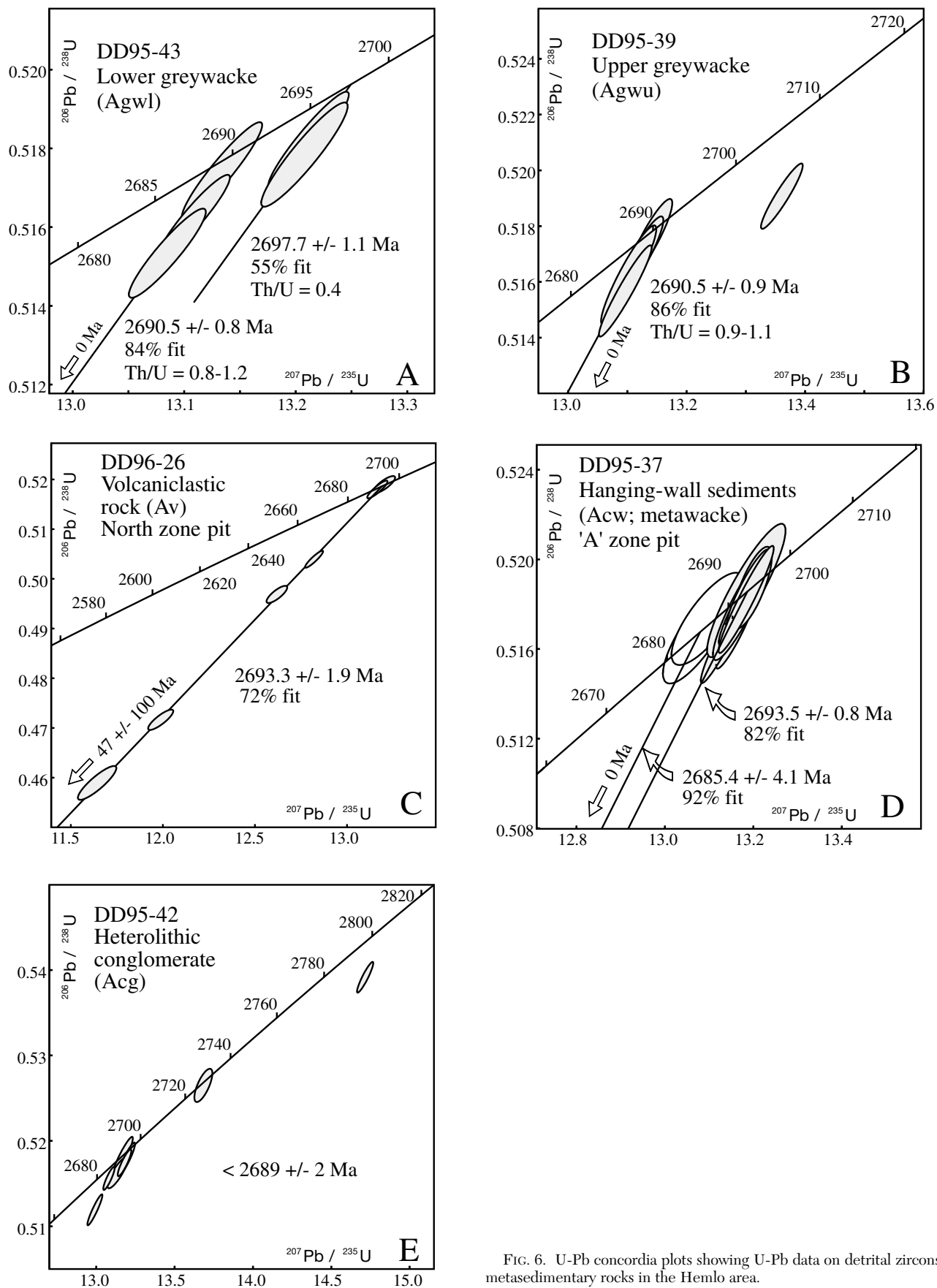


FIG. 6. U-Pb concordia plots showing U-Pb data on detrital zircons from metasedimentary rocks in the Hemlo area.

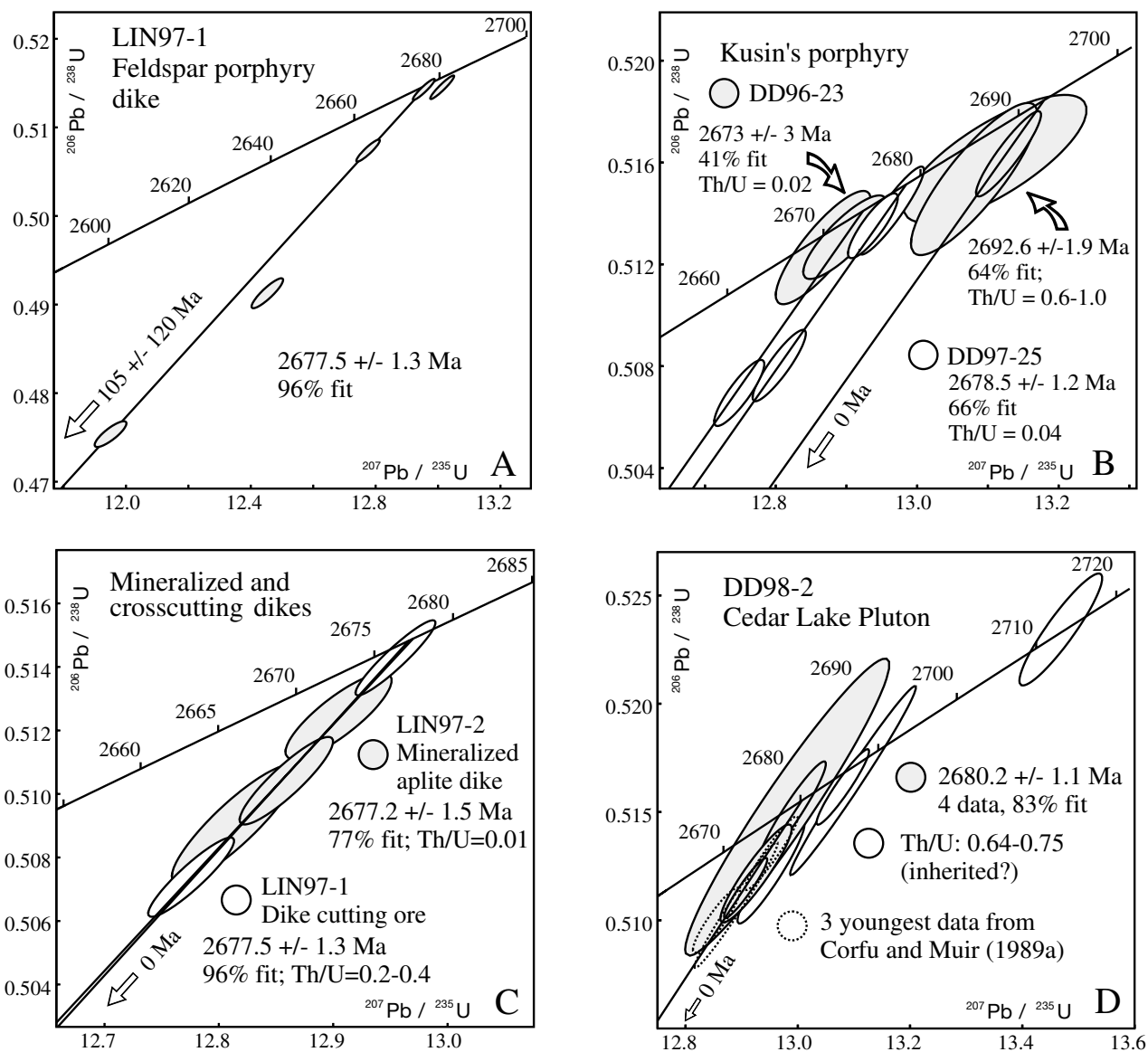


FIG. 7. U-Pb concordia plots showing data on single zircons from dikes and the Cedar Lake pluton in the Hemlo area.

Metasedimentary samples

DD95-43 Lower graywacke east of the deposit, map unit Agwl (Fig. 6A): This sample was from an extensive group of metasedimentary outcrops along the highway east of the mine area. The rocks are mostly rather fine grained with graded beds. Zircons in this sample show a rather uniform, euhedral morphology (Fig. 4B). Five single grains were analyzed, and these give concordant or near-concordant data. They define two clusters, one with an average age of 2690.5 ± 0.8 Ma, the other with an age of 2697.7 ± 1.1 Ma. The calculated Th/U ratios of the 2691 Ma zircons are relatively high (0.8–1.2; Table 1), compared to those of the two older, 2698 Ma zircons (0.4).

DD95-39 Upper graywacke, map unit Agwu (Fig. 6B): The zircons make up a uniform-looking population of colorless euhedral and subrounded grains, with relatively few well rounded grains. Analyses of two euhedral and two subrounded

single grains are concordant, or nearly so, and have ages that are well within error. The average $^{207}\text{Pb}/^{206}\text{Pb}$ age is 2690.5 ± 0.9 Ma. This is an older age limit on deposition of the sediment, which appears to have been derived from a rather uniform source. Analysis of a single, well rounded zircon gave a slightly discordant datum with an older age of 2713 ± 2 Ma. The younger zircons from this sample agree in age with the younger zircons from the lower graywacke (DD95-43), and have similarly high Th/U ratios (0.9–1.6).

DD96-26 Reworked felsic volcanoclastic rock at the North zone pit, map unit Av (Fig. 6C): The sample yielded small, stubby to elongate, euhedral to subrounded zircons, many of which are fresh (Fig. 4C). Some grains are rounded and frosted, suggesting that they may be detrital contaminants. Yellow to brown rutile is present in the magnetic separates. Analyses of six euhedral zircons yielded four discordant and two concordant data. The discordance is probably caused by

a bad batch of column resin, which produced excess U blanks. Because of the small sample sizes, only a few picograms of excess U would cause significant apparent discordance. However, all data show overlapping $^{207}\text{Pb}/^{206}\text{Pb}$ ages with an average of 2693.3 ± 1.9 Ma. This is an older age limit on deposition of the sedimentary unit. The euhedral population was likely derived from an almost uniform source that records late volcanism.

DD95-37 Hanging-wall metasediment (calc-silicate-rich metawacke) at A zone pit, map unit Acw (Fig. 6D): This sample contained a moderate amount of barite, from which zircons were separated by hand picking. The zircons are generally fresh but small. Stubby euhedral to subrounded grains make up most of the population. Only euhedral zircons were analyzed, and these gave concordant data. Averaging the $^{207}\text{Pb}/^{206}\text{Pb}$ ages of all data gives an age of 2693.2 ± 0.7 Ma with only a 10 percent probability of fit. The data can be divided into two discrete clusters. Averaging the $^{207}\text{Pb}/^{206}\text{Pb}$ ages of the ten older data defines an age of 2693.5 ± 0.8 Ma with an 82 percent probability of fit. The two younger data define an age of 2685.4 ± 4.1 Ma with a 92 percent probability of fit. Unfortunately, these two grains had low uranium concentrations so their data points are relatively imprecise. However, the mass spectrometer data are of excellent quality, and their age difference from the older data cluster appears to be resolved. The two younger concordant data provide an older age limit for sediment deposition, of 2685 ± 4 Ma.

DD95-42 Heterolithic conglomerate, map unit Acg (Fig. 6E): Detrital zircon ages from the conglomerate are clustered around ca. 2690 Ma, with one much older grain at 2810 Ma. This is approximately the same range of ages as that of zircons dated from the underlying porphyry and metasedimentary rocks, and supports field interpretations that the conglomerate was at least partly derived from the rocks that presently underlie it. In all previous studies, ca. 2800 Ma age zircons have only been found in the Moose Lake porphyry. This is consistent with the interpretation that quartz porphyry clasts observed in the conglomerate were derived from the Moose Lake porphyry (Lin, 2001a). An older age limit on deposition of the conglomerate is given by the youngest zircons, at 2689 ± 2 Ma.

Dike and pluton samples

LIN97-1 Feldspar porphyry dike cutting ore (Fig. 7A): This sample was taken from the dike shown in figure 11 of Lin (2001a). It is observed to cut the ore and is not mineralized, as is generally true for feldspar porphyry dikes in the area (Lin, 2001a, fig. 27A–C). The sample yielded only a small amount of zircon, generally as highly cracked brown euhedral grains and fragments (Fig. 4D). In contrast to samples from the metavolcanic and metasedimentary rocks, the zircon population shows a high proportion of long-prismatic grains with well developed, low-order prism faces similar to morphological type G1 defined by Pupin (1980). Five zircons were analyzed, but these produced only two data near concordia, which do not agree in age. The youngest concordant datum gives an age of 2677 ± 2 Ma. This is an older age limit on emplacement of the dike. It is consistent with two discordant data, giving a well defined regression with an upper concordia intercept age of 2677.5 ± 1.3 Ma and a lower intercept

within error of zero. This is the best estimate for the age of emplacement of the dike. The two other data are slightly older and probably contain inheritance. One of these, an unusual flat zircon, shows a very low Th/U ratio but must be a xenocryst, based on its older, 2684 ± 2 Ma age.

DD96-23 and DD97-25 Kusin's porphyry (Fig. 7B): Two samples were processed from this feldspar porphyry intrusion, shown in figure 23 (“+” fill) of Lin (2001a). Only a small amount of zircon was recovered from both samples as tiny fragments and euhedral, long-prismatic grains. The zircons are generally quite cracked, and there was very little material that could be reliably dated. This unit clearly contains inherited zircons, as shown by a 2779 Ma age. Three concordant to near-concordant data from DD96-23 overlap and define an age of 2692.6 ± 1.9 Ma. Two other concordant data from this sample define a distinctly younger age of 2673 ± 3 Ma. Two concordant data from DD97-25 and a slightly discordant datum have overlapping $^{207}\text{Pb}/^{206}\text{Pb}$ ages with an average of 2679 ± 1 Ma. The Th/U ratio of all the younger zircons is extremely low (0.02; Table 1). This suggests that the younger zircon may be metamorphic or hydrothermal in origin, especially since a whole-rock sample of DD96-23 gave a normal Th/U ratio of 2.3.

LIN97-2 Mineralized aplite dike (Fig. 7C): This sample, taken from the mineralized dike shown in figure 26A of Lin (2001a), yielded a small amount of pale-brown, euhedral, long-prismatic zircon (Fig. 4E), similar in appearance to that from the other dikes. Three single zircons that are typical of the population gave near-concordant data with overlapping $^{207}\text{Pb}/^{206}\text{Pb}$ ages. These define an age of 2677 ± 2 Ma (77% probability of fit). All of the zircon analyses show very low Th/U ratios. However, the Th/U ratio of the whole rock is also low (0.2).

DD98-2 Granodiorite, Cedar Lake pluton, map unit Agd (Fig. 7D; sample location shown in Fig. 1): Zircon is abundant in this sample, but the grains are mostly quite cracked. The morphology is typically short prismatic, with well developed secondary faces. Uncracked, whole euhedral grains were picked for abrasion (Fig. 4F). Six of these were analyzed, as well as three fragments that had been broken off the tips of grains and abraded. Two analyses give overlapping concordant data with an average age of 2688 ± 1 Ma, the previously assigned age for this pluton. However, five other data are younger, whereas one analysis produced an older age. The four youngest data, including those from the three tips, give overlapping $^{207}\text{Pb}/^{206}\text{Pb}$ ages with an average of 2680.2 ± 1.1 Ma. These analyses show Th/U ratios in the range of 0.35 to 0.45, which is consistently lower than that of the older analyses, but still within the normal range for igneous zircon. The most conservative interpretation is that the 2680 Ma zircon population gives an older age limit on igneous crystallization of the pluton.

Discussion

Age constraints on stratigraphy

Rocks of the Moose Lake porphyry (map unit AMLp) show abundant zircon inheritance with a variety of ages extending back to 2816 Ma (Fig. 5A–C). Ages around 2800 Ma were found in all three dated samples of the porphyry and must

reflect an older source with which these magmas interacted. The previously published age of 2772 ± 2 Ma, by Corfu and Muir (1989a), is probably an artifact of mixing inheritance ages in multigrain fractions, which it was necessary to analyze at the time because of higher blank levels. The youngest datum from the mineralized fragmental unit (DD95-38) gives an age of 2694 ± 2 Ma. The porphyry from the Barren Sulfide zone (DD95-41) has younger, although slightly more discordant, zircons at 2688 ± 2 Ma. Thus, an older age limit for emplacement, based on data from the porphyry itself, is 2691 ± 5 Ma.

The quartz porphyry from south of the Hemlo fault (DD95-44, map unit Afs) was emplaced after 2699 ± 1 Ma and also shows abundant inheritance, principally from a source 2723 ± 1 Ma in age, as defined by 3 data (Fig. 5D). Two zircon grains from the mineralized fragmental unit (DD95-38) show a similar inheritance age of 2722 ± 1 Ma (Fig. 5A). Although the significance of inherited ages is uncertain because of the possibility of partial resetting and core-overgrowth mixing, this is approximately the age of gneiss from the underlying Pukaskwa intrusive complex south of the Hemlo area (Corfu and Muir, 1989a; Fig. 1). In terms of its age constraint and complex inheritance pattern, this porphyry resembles phases of the Moose Lake porphyry, although evidence for the ca. 2800 Ma inherited age component is, thus far, lacking.

The metasedimentary rocks contain abundant detrital zircons that appear to be from rather uniform sources. The sample from the lower graywacke (DD95-43, map unit Agwl) contains a zircon population with an age of 2690.5 ± 0.8 Ma (Fig. 6A). A similar zircon population with an age of 2690.5 ± 0.9 Ma (Fig. 6B) is present in the upper graywacke (DD95-39, map unit Agwu), which overlies the Moose Lake porphyry. These similarly aged zircons, along with their distinctive high Th/U ratios, suggest that the sedimentary provenance of the zircons remained unchanged before and after deposition of the Moose Lake porphyry, although the upper graywacke is more mafic and contains abundant magnetite bands near its base.

The reworked volcanoclastic rocks at North zone (DD96-26, map unit Av) also seem to preserve a relatively uniformly aged, euhedral zircon population, but the age of 2693.3 ± 1.9 Ma (Fig. 6C) is different from that in the upper and lower graywackes. Ten euhedral zircons in the hanging-wall metasedimentary rock (DD95-37, map unit Acw) define a similar age as that found in the reworked volcanoclastic rocks (2693.5 ± 0.8 Ma; Fig. 6D). The abundance of 2693 Ma zircons with similar morphology and Th/U ratios in both samples supports the field interpretation of Lin (2001a) that the reworked volcanoclastic rocks (unit Av) and the hanging-wall calc-silicate-rich metasediment (unit Acw) are stratigraphic equivalents. Two zircons from the hanging-wall metasediment yield younger concordant data with an age of 2685 ± 4 Ma. This should be an older age estimate on deposition of the metasedimentary rock and overlying units, as well as on gold mineralization.

Muir (1997) suggested that the reworked volcanoclastic material could have been derived from the Moose Lake porphyry. Although three zircons from the Barren Sulfide zone porphyry and one from the mineralized porphyry gave ages within error of zircons in the volcanoclastics, these rocks have

yielded no evidence for older zircon xenocrysts (2720–2810 Ma), although they are abundant in the porphyry. There is also no apparent overlap with ages of zircon detritus in the upper and lower graywackes, despite the fact that these units are interpreted to stratigraphically bracket the volcanoclastics. It seems that the volcanoclastic and calc-silicate band units were derived from a 2693 Ma volcanic formation that temporarily dominated the provenance of the basin until it eroded away and background provenance from a slightly younger, 2691 Ma source became reestablished. The 2685 ± 4 Ma average age on the two youngest detrital zircons from the hanging-wall metasediment (Fig. 6D), although relatively imprecise, suggests that all dated zircons in the overlying Moose Lake porphyry are xenocrystic, except perhaps for the youngest (2688 ± 2 Ma) zircons in the sample from the Barren Sulfide zone.

The general uniformity of provenance ages for the individual metasedimentary units suggests that they had a local source, and the fact that these ages predate sediment deposition by only a few million years suggests that the setting was a volcanically active sedimentary basin. The volcanic rocks apparently erupted through ca. 2,720 million-year-old rocks, which are typical of early phases in the Hemlo belt (Corfu and Muir, 1989a; Jackson et al., 1998) and the Manitouwadge belt to the north (Zaleski et al., 1999). The final episode of volcanism was eruption of the Moose Lake porphyry, zircons of which appear to be mostly xenocrystic. The Moose Lake porphyry sampled older, ca. 2800 Ma rocks, which do not appear to have been exposed to erosion. These rocks were folded and unconformably overlain by a locally derived conglomerate and carbonate unit. The youngest zircons in the conglomerate are similar in age to those from underlying metasedimentary rocks (ca. 2690 Ma) and do not help to further constrain the age of deposition.

Age constraints on deformation, metamorphism, and gold mineralization

In order to directly constrain the timing of gold mineralization, zircons were analyzed from three dike samples. One concordant and two discordant data from a feldspar porphyry dike that cuts gold ore (LIN97-1) define an age of 2677.5 ± 1.3 Ma (Fig. 7A). The Th/U ratios of these zircons overlap with the range typically found in magmatic rocks, so they are probably not metamorphic or hydrothermal in origin. Therefore, this result is interpreted as a minimum age estimate on gold. It is similar to the age of regional, late-tectonic plutonism represented by the Gowan Lake pluton dated at 2678 ± 2 Ma by Corfu and Muir (1989a), and suggests the possibility that a similarly aged pluton underlies that area of the gold deposit.

The Kusin's feldspar porphyry (DD96-23 and DD97-25) also cuts ore. Relatively young, low-Th/U (<0.05) populations of zircons from two samples give ages of 2673 ± 3 and 2679 ± 1 Ma (Fig. 7B). The youngest datum agrees with the 2671 ± 2 Ma age measured on metamorphic titanite from dikes and schists within the deposit (Corfu and Muir, 1989b), whereas the 2679 ± 1 Ma age is in agreement with titanite from regional metamorphism outside the deposit (Corfu and Muir, 1989a; Jackson et al., 1998). Considering that the whole-rock samples show normal Th/U ratios (>2), it is likely that the

young generations of zircon did not crystallize from a magma, but are metamorphic or hydrothermal in origin. Three other concordant data from one of the samples define an age of 2693 ± 2 Ma. These are similar in age to zircons in the adjacent hanging-wall sediments (DD95-37), and are likely to be xenocrysts. The ca. 2693 Ma zircons from the Kusun's porphyry have substantially higher Th/U (0.6–1.0) than the 2677 Ma zircons in the feldspar porphyry dike (LIN97-1; Th/U of 0.2–0.4), even though the whole-rock Th/U of the Kusun's porphyry sample is lower than that of the feldspar porphyry dike sample (2.3 vs. 3.0, respectively). Since these rocks are of similar mineral and chemical composition, there is no reason to expect their zircons to have different trace-element partition coefficients with the magma, so the ca. 2693 Ma zircons from the Kusun's porphyry are probably inherited.

The aplite dike (LIN97-2) is mineralized (5 g/t of gold), although there is some controversy as to whether the mineralization is primary (Robert and Poulsen, 1997; Lin, 2001a). The dike is folded by F_2 and contains a strong S_2 foliation (see Lin, 2001a, fig. 26). It either predated or was synchronous with G_2 deformation and is interpreted by Lin (2001a) to have either predated or been synchronous with primary mineralization. The zircons define an age of 2677.2 ± 1.5 Ma, similar to the ore-cutting feldspar porphyry dike (Fig. 7C). These zircons show very low Th/U, which may be an indication that they are metamorphic in origin. However, chemical analysis of LIN97-2 also shows a low whole-rock Th/U of 0.2, substantially below that of most nonaplitic or pegmatitic igneous rocks. This is permissive evidence that the zircons are magmatic and that gold mineralization took place at 2677 ± 1 Ma. Unfortunately, this cannot be tested independently.

Problems with interpreting the paragenesis of zircon become obvious when single grains are precisely dated. Multi-grain zircon fractions such as those analyzed in early work by Corfu and Muir (1989a) would be susceptible to partial contamination from xenocrystic and metamorphic grains, although results may tend to average out, giving overlapping ages for different fractions. The present sample of the Cedar Lake pluton shows zircon ages at 2688 Ma, the previously accepted age of the pluton, 2713 Ma, and 2680 ± 1 Ma (Fig. 7D). The younger zircon results are consistent with overlapping $^{207}\text{Pb}/^{206}\text{Pb}$ ages from the youngest near-concordant data measured by Corfu and Muir (1989a) on an internal phase of the Cedar Lake pluton (sample CL1, analyses 19–21 of Corfu and Muir, 1989a). These average to 2680.4 ± 1.0 Ma with a marginally acceptable probability of fit (18%), and are plotted on Figure 7D. Combining the seven youngest near-concordant data from both samples gives an average $^{207}\text{Pb}/^{206}\text{Pb}$ age of 2680.3 ± 0.8 Ma with a 63 percent probability of fit. A similar argument can be made that emplacement of the other major intrusion in the area, the Heron Bay pluton, was no earlier than 2682 ± 2 Ma (samples HBm and Hbi, analyses 38 and 39 of Corfu and Muir, 1989a). All of these analyses show Th/U ratios that fall within the range of magmatic zircon. Many of the 2685 to 2688 Ma age interpretations in Corfu and Muir (1989a) were strongly based on the assumption that abraded zircons were affected by a Keweenaw Pb-loss event related to emplacement of the nearby Coldwell Complex at about 1100 Ma. Although some discordant data from unabraded fractions do define ca. 1100 Ma lower concordia

intercepts, near-concordant (<2% discordant) data from abraded fractions in studies where there is independent age control (e.g., Davis and Green, 1997) are generally found to record only recent Pb loss. Therefore $^{207}\text{Pb}/^{206}\text{Pb}$ ages from such zircons are normally expected to give a reliable estimate of their crystallization ages. Given the complexity in zircon systematics that we now know to be present in the Hemlo area, there is a high probability that multigrain analyses from many rocks would be affected by inheritance. This is especially clear in the case of the Moose Lake porphyry as discussed above. Subtle inheritance might be less evident, but would tend to bias ages toward older values, a problem exacerbated by forcing discordant data through Pb loss lines with old lower intercepts. Thus, data from the Corfu and Muir (1989a) study are consistent with the present interpretation that the Cedar Lake pluton formed from melting of slightly older felsic crust and that its emplacement occurred no earlier than 2680 ± 1 Ma.

The Cedar Lake pluton intruded before or early during G_2 , and the feldspar porphyry dikes late during G_2 (Lin, 2001a). Therefore, at least a significant part of G_2 deformation took place between 2680 ± 1 and 2677.5 ± 1.3 Ma (age of the feldspar porphyry dike). Regional metamorphism postdates gold mineralization and occurred either late during G_2 deformation or after it (Lin, 2001a). A younger age limit on peak regional metamorphism is probably given by the 2676 Ma age of titanite outside the deposit (Corfu and Muir, 1989b; D.W. Davis, unpub. data). These data constrain G_2 deformation and peak regional metamorphism as part of a rather short-lived event that culminated with emplacement of late tectonic intrusions, such as the 2678 ± 2 Ma Gowan Lake pluton (Corfu and Muir 1989a; Beakhouse, 2001). Lin (2001a) concludes that primary gold mineralization occurred before or early during G_2 deformation. If it occurred before G_2 , it could have been as early as 2685 ± 4 Ma, the age of the youngest zircons in the supracrustal rocks. If it occurred early during G_2 , as is most likely the case based on field evidence (Lin, 2001a), it likely occurred between emplacement of the Cedar Lake pluton at 2680 ± 1 Ma and the age of the ore-cutting dikes at 2677 ± 1 Ma.

Implications of geochronology for the origin and setting of the Hemlo gold deposit

The present data outline a ca. 15-m.y. period of progressive geologic development that included formation and erosion of a volcanic complex, plutonism, mineralization, major crustal deformation, and metamorphism (Fig. 8). The postvolcanic part of this process is constrained to a shorter time span of ca. 2682 to 2676 Ma, during which large volumes of granitoid magma were injected into a deforming crust. The close time association supports previous suggestions, based on alteration mineral assemblage and metal abundance of the deposit, that granitoid magmas were the source of the mineralizing fluids (e.g., Burk, 1987; Kuhns, 1988). The large felsic plutons were probably also a major heat source for regional metamorphism. The evolution of these granitoid magmas from an early calc-alkaline (Cedar Lake-type) suite dominated by crustal contamination to a later mantle-derived sanukitoid (Gowan Lake-type) suite suggests that an increasingly deeper melt source became dominant with time (Beakhouse, 2001).

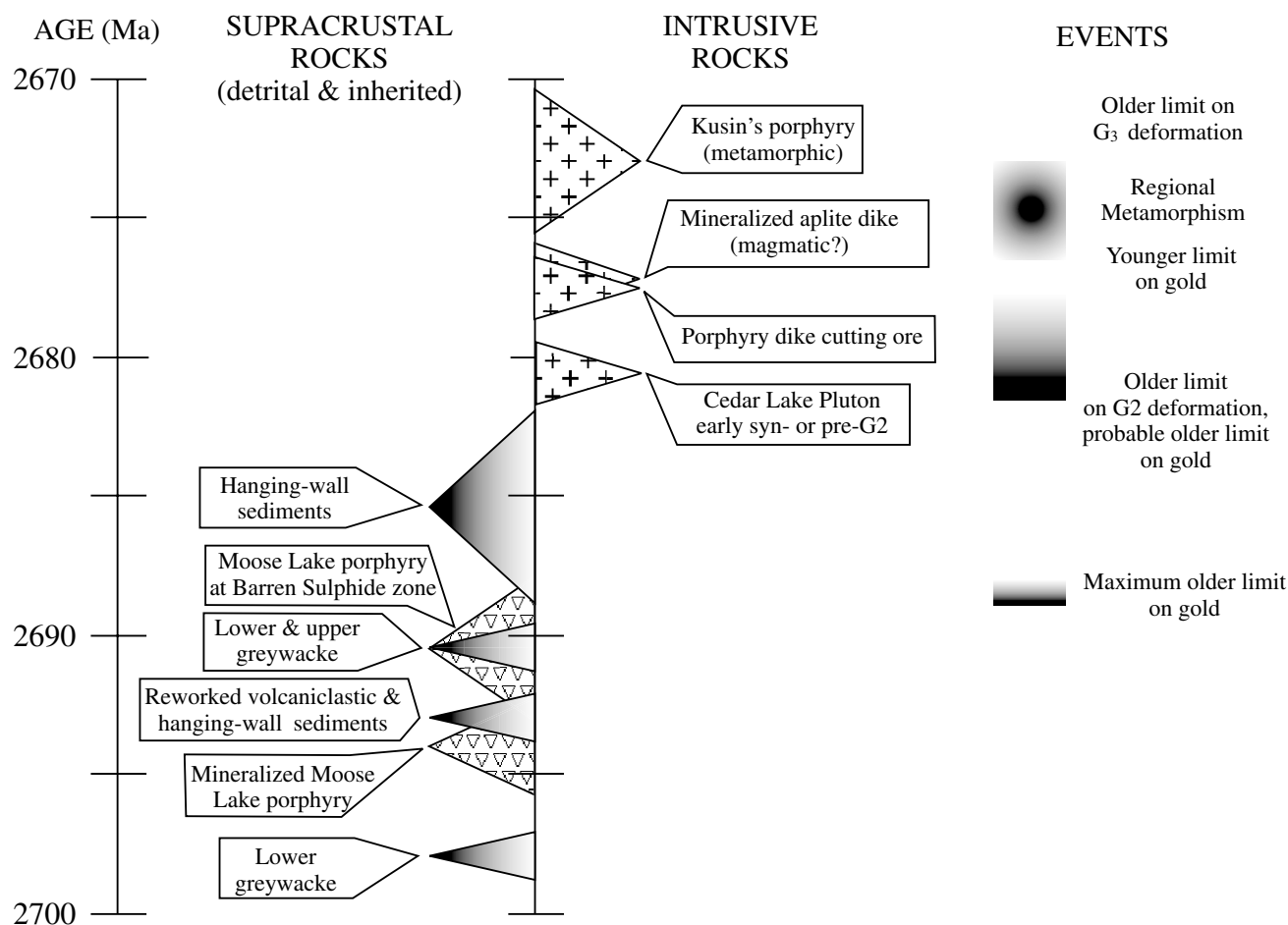


FIG. 8. Summary of age constraints in the Hemlo gold camp. Shading in the right-hand column gives a rough estimate of confidence levels in the age constraints on major geologic events.

The sanukitoid suite defined by Shirey and Hanson (1984) contains rocks that show high levels of both compatible and incompatible elements, apparently because their mantle source was metasomatically enriched prior to melting.

The conglomerate and cummingtonite schist unconformably overly folded rocks and are themselves intensely deformed by G_2 folds and fabrics (Lin, 2001a). This, along with the rapidity of development of the volcanosedimentary sequence, uniform provenance, and localization along a major regional shear zone suggests that deposition was in a tectonically as well as volcanically active basin where sediments were progressively deposited, buried, and folded by ongoing deformation. Rock packages showing similar relationships have been found elsewhere in the Superior province and are known as Timiskaming-type sequences (Mueller and Donaldson, 1992). Such rocks may have been deposited in late orogenic, fault-controlled basins that formed in local extensional (pull-apart) environments or as a result of thrusting. They characteristically contain fluviatile and deep-water sediments associated with calc-alkaline and alkalic volcanism, which quickly eroded into the basin and were deformed in a transpressional tectonic regime. Timiskaming-associated rocks are hosts to some of the largest Archean gold deposits, particularly those

localized along major faults in the southern Abitibi greenstone belt (Corfu et al., 1991; Mueller et al., 1996). Deposition in these areas was ongoing at 2680 to 2677 Ma (Corfu et al., 1991; Mueller et al., 1996), an age range similar to the period of mineralization, deformation, and metamorphism at Hemlo. Hemlo seems to show a more precocious development than Timiskaming systems in the southern Abitibi belt. Perhaps this is because it represents a deeper crustal exposure of such systems.

Leclair et al. (1993) suggested that auriferous shear zones such as the Porcupine-Destor fault may be traceable over large distances through different metamorphic terranes in the Superior province. Lin (1998) noted some similarities in geological settings between the Hemlo deposit and the Dome mine in Timmins. Mineralized porphyries in the Timmins area along the Porcupine-Destor fault have similar ca. 2690 Ma ages to zircons commonly found in sediments at Hemlo (Corfu et al., 1989). The Shebandowan greenstone belt to the west of Hemlo also contains evidence for Timiskaming-type sedimentation in the age range of 2690 to 2680 Ma (Corfu and Stott, 1998). If these areas represent eastern and western extensions of the lithotectonic environment found at Hemlo, they potentially contain other Hemlo-type gold deposits.

Conclusions

Gold mineralization at Hemlo was preceded by development of a volcanosedimentary complex built upon an older greenstone basement. Detrital and xenocrystic zircon ages tend to cluster around 2810, 2722, 2698, 2693, and 2691 Ma and may record significant magmatic events in the Hemlo area. The Moose Lake porphyry is highly contaminated from ca. 2800 Ma and younger sources, whereas the associated metasedimentary rocks appear to contain a significant component of ca. 2690 Ma detrital zircon. The youngest age from supracrustal rocks is 2685 ± 4 Ma from two detrital zircons.

Granitoid plutonism, gold mineralization, major deformation, and metamorphism are bracketed within the age range of 2681 to 2676 Ma, based on ages from the Cedar Lake pluton, metamorphic zircon, and a dike that cuts ore. Thus, granitoid magmas may have been the source of mineralizing fluids as well as a principal heat source for metamorphism. Major ductile deformation in the crust and granitoid magmatism were effectively coeval. Gold at Hemlo was probably emplaced into a Timiskaming-type sedimentary basin during its latest, most intense stage of tectonic development.

Acknowledgments

Richard Sutcliffe is acknowledged for leading the multidisciplinary CAMIRO project that commissioned this study, as well as for continuing advice and support. Interpretations have greatly benefited from conversations with Steve Jackson and Gary Beakhouse of the Ontario Geological Survey. The Canadian Mining Industry Research Organization, particularly Ed Debicki, and participating companies are thanked for their foresight in supporting research.

Raivo Tahiste, Tom Pestaj, and Vicki Abboud carried out crushing and sample processing. Galina Amelina assisted in analytical work. Bohdan Podstawskyj maintained the mass spectrometer. Whole-rock Th/U analyses were carried out at the Ottawa laboratories of the Geological Survey of Canada.

Thanks are given to Rodney Allen, Kjell Billstrom, Mark Hannington, and especially to Tom Muir for carefully reviewing the manuscript. These reviews greatly improved the quality of the manuscript.

February 19, October 21, 2002

REFERENCES

- Beakhouse, G.P., 2001, Nature timing and significance of intermediate to felsic intrusive rocks associated with the Hemlo greenstone belt and implications for the regional geological setting of the Hemlo gold deposit: Ontario Geological Survey, Open File Report 6020, 248 p.
- Burk, R.L., 1987, Geological setting of the Teck-Corona gold-molybdenum deposit, Hemlo, Ontario: Unpublished M.Sc. thesis, Kingston, Ontario, Queen's University, 241 p.
- Corfu, F., and Davis, D.W., 1991, Comment on the paper Archean hydrothermal zircon in the Abitibi greenstone belt: Constraints on the timing of gold mineralization: *Earth and Planetary Science Letters*, v. 104, p. 545–552.
- Corfu, F., and Muir, T.L., 1989a, The Hemlo-Heron Bay greenstone belt and Hemlo Au-Mo deposit, Superior province, Canada. 1: Sequence of igneous activity determined by zircon U-Pb geochronology: *Chemical Geology (Isotope Geoscience Section)*, v. 79, p. 183–200.
- 1989b, The Hemlo-Heron Bay greenstone belt and Hemlo Au-Mo deposit, Superior province, Canada. 2: Timing of metamorphism, alteration, and Au mineralization from titanite, rutile, and monazite U-Pb geochronology: *Chemical Geology (Isotope Geoscience Section)*, v. 79, p. 201–223.
- Corfu, F., and Stott, G.M., 1998, The Shebandowan greenstone belt, western Superior province: U-Pb ages, tectonic implications, and correlations: *Bulletin of the Geological Society of America*, v. 110, p. 1467–1484.
- Corfu, F., Krogh, T.E., Kwok, Y.Y., and Jensen, L.S., 1989, U-Pb geochronology in the southwestern Abitibi greenstone belt, Superior province: *Canadian Journal of Earth Sciences*, v. 26, p. 1747–1763.
- Corfu, F., Jackson, S.L., and Sutcliffe, R.H., 1991, U-Pb ages and tectonic significance of late Archean alkalic magmatism and non-marine sedimentation: Timiskaming Group, southern Abitibi belt, Ontario: *Canadian Journal of Earth Sciences*, v. 28, p. 489–503.
- Davis, D.W., 1982, Optimum linear regression and error estimation applied to U-Pb data: *Canadian Journal of Earth Sciences*, v. 19, p. 2141–2149.
- Davis, D.W., and Green, J.C., 1997, Geochronology of the North American Midcontinent Rift in western Lake Superior and implications for its geodynamic evolution: *Canadian Journal of Earth Sciences*, v. 34, p. 476–488.
- Goldie, R., 1985, The sinters of the Ohaki and Champagne pools, New Zealand: Possible analogues of the Hemlo gold deposit, Northern Ontario: *Geoscience Canada*, v. 12, p. 60–64.
- Hugon, H., 1986, The Hemlo gold deposit, Ontario, Canada: A central portion of a large-scale, wide zone of heterogeneous ductile shear, in MacDonald, A.J., ed., *Gold '86: Willowdale, Ontario*, Konsult International, p. 379–387.
- Jackson, S.L., Beakhouse, G.P., and Davis, D.W., 1998, Regional geological setting of the Hemlo gold deposit: An interim progress report: Ontario Geological Survey, Open File Report 5977, 151 p.
- Jaffey, A.H., Flynn, K.F., Glendenin, L.E., Bentley, W.C., and Essling, A.M., 1971, Precision measurement of half-lives and specific activities of ^{235}U and ^{238}U : *Physical Review*, v. 4, p. 1889–1906.
- Johnston, P., 1996, The geological setting of the Hemlo gold deposit: Unpublished Ph.D. thesis, Kingston, Ontario, Queen's University, 297 p.
- Johnston, P., and Smyk, M.C., 1992, The anatomy of the Hemlo Au-Mo deposit, Ontario [abs.]: Geological Association of Canada Annual Meeting, Wolfville, Nova Scotia, Acadia University, May 25–27, Program with Abstracts, v. 17, p. A53.
- Krogh, T.E., 1973, A low contamination method for hydrothermal decomposition of zircon and extraction of U and Pb for isotopic age determinations: *Geochimica et Cosmochimica Acta*, v. 37, p. 485–494.
- 1982, Improved accuracy of U-Pb ages by the creation of more concordant systems using an air abrasion technique: *Geochimica et Cosmochimica Acta*, v. 46, p. 637–649.
- Krogh, T.E., and Davis, G.L., 1974, Alteration in zircons with discordant U-Pb ages: *Carnegie Institution of Washington Yearbook*, v. 73, p. 560–567.
- 1975, Alteration in zircons and differential dissolution of altered and metamict zircon: *Carnegie Institution of Washington Yearbook*, v. 74, p. 619–623.
- Kuhns, R.J., 1988, The Golden Giant deposit, Hemlo, Ontario: Geologic and geochemical relationships between mineralization, alteration, metamorphism, magmatism, and tectonism: Ph.D. thesis, Minneapolis, University of Minnesota, 458 p.
- Kuhns, R.J., Sawkins, F.J., and Ho, E., 1994, Magmatism, metamorphism, and deformation at Hemlo, Ontario, and the timing of Au-Mo mineralization in the Golden Giant mine: *ECONOMIC GEOLOGY*, v. 89, p. 720–756.
- Leclair, A.D., Ernst, R.E., and Hattori, K., 1993, Crustal-scale auriferous shear zones in the central Superior province, Canada: *Geology*, v. 21, p. 399–402.
- Lin, S., 1998, Structural setting of the Hemlo gold deposit, Ontario: Geological Survey of Canada Paper 1998-E, p. 77–88.
- 2001a, Stratigraphic and structural setting of the Hemlo gold deposit, Ontario, Canada: *ECONOMIC GEOLOGY*, v. 96, p. 477–507.
- Lin, S., 2001b, Geology, the Hemlo gold camp, Ontario: Geological Survey of Canada Map 1975A, scale 1:10,000, with sections and plans at a scale of 1:2,000.
- Ludwig, K.R., 1998, Using ISOPLOT/Ex version 1.00b—a geochronological toolkit for Microsoft Excel: Berkeley Geochronology Center Special Publication 1, 43 p.
- Mueller, W., and Donaldson, J.A., 1992, Development of sedimentary basins in the Archean Abitibi belt, Canada: An overview: *Canadian Journal of Earth Sciences*, v. 29, p. 2249–2265.
- Mueller, W.U., Daigneault, R., Mortensen, J.K., and Chown, E.H., 1996, Archean terrane docking: Upper crust collision tectonics, Abitibi greenstone belt, Quebec, Canada: *Tectonophysics*, v. 265, 127–150.
- Muir, T.L., 1993, The geology of the Hemlo gold deposit area: Ontario Geological Survey Open File Report 5877, 264 p.

- 1997, Precambrian geology, Hemlo deposit area: Ontario Geological Survey Report 289, 219 p.
- Muir, T.L., and Elliott, C.G., 1987, Hemlo tectono-stratigraphic study, District of Thunder Bay: Ontario Geological Survey Miscellaneous Paper 137, p. 117–129.
- Muir, T.L., Schnieders, B.R., and Smyk, M.C., eds., 1991, Geology and gold deposit of the Hemlo area: Geological Association of Canada-Mineralogical Association of Canada-Society of Economic Geologists, Joint Annual Meeting, Toronto, Canada, 1991, Field Trip A1 Guidebook, 106 p.
- Pan, Y., and Fleet, M.E., 1995, The late Archean Hemlo gold deposit, Ontario, Canada: A review and synthesis: *Ore Geology Reviews*, v. 9, p. 227–229.
- Powell, W.G., Pattison, D.R.M., and Johnston, P., 1999, Metamorphic history of the Hemlo gold deposit from Al_2SiO_5 mineral assemblages, with implications for the timing of mineralization: *Canadian Journal of Earth Sciences*, v. 36, p. 33–46.
- Pupin, J.P., 1980, Zircon and granite petrology: *Contributions to Mineralogy and Petrology*, v. 73, p. 207–220.
- Robert, F., and Poulsen, K.H., 1997, World-class Archean gold deposits in Canada: An overview: *Australian Journal of Earth Sciences*, v. 44, p. 329–351.
- Rubatto, D., 2002, Zircon trace element geochemistry: partitioning with garnet and the link between U-Pb ages and metamorphism: *Chemical Geology*, v. 184, p. 123–138.
- Shirey, S.B., and Hanson, G.N., 1984, Mantle-derived Archean monzodiorites and trachyandesites: *Nature*, v. 310, p. 222–224.
- Sutcliffe, R.H., Morris, W.A., Reed, L.E., Lin, S., Williams-Jones, A.E., Davis, D.W., Manning, S., LeBlanc, G., Bodycomb, V., Clark, J.R., and Heiligmann, M., 1998, Finding the next Hemlo: Defining the parameters: CAMIRO Exploration Division Hemlo Research Project, Final Report, April 30, 1998, v. 1, 37 p.
- Valliant, R.L., and Bradbrook, C.J., 1986, Relationship between stratigraphy, faults, and gold deposits, Page-Williams mine, Hemlo, Ontario, Canada, in MacDonald, A.J., ed., *Gold '86: Willowdale, Ontario*, Konsult International, p. 355–361.
- Zaleski, E., van Breemen, O., and Peterson, V.L., 1999, Geological evolution of the Manitowadge greenstone belt and Wawa-Quetico subprovince boundary, Superior province, Ontario, constrained by U-Pb zircon dates of supracrustal and plutonic rocks: *Canadian Journal of Earth Sciences*, v. 36, p. 945–966.